IJCRT.ORG ISSN : 2320-2882

INTERNATIONAL JOURNAL OF CREATIVE RESEARCH THOUGHTS (IJCRT)

An International Open Access, Peer-reviewed, Refereed Journal

A Comprehensive Investigation On Ethyl 2-((3-Methyl-1-Phenyl-1H-Pyrazol-5-Yl Oxy) (4-(Trifluoromethyl) Phenyl) Methyl: Photophysical And Biological Application

S.M. Nimbalagundi[1] and S.N. Poleshi[1*]

M.G.V.C.Arts Commerce and Science College Muddebihal District Vijayapur, Karnataka , India

Abstract:

In the present work, aryl-substituted pyrazolones derivative *Ethyl 2-((3-methyl-1-phenyl-1H-pyrazol-5-yl oxy) (4-(triflurомethyl) phenyl) methyl)acrylate* (ETH) have been synthesized by the reaction of Baylis-Hillman acetate with pyrazolones and screened for their *in vitro* antifungal, antibacterial and antioxidant properties. The molecule shows good *in vitro* antifungal and antibacterial activities due to the presence of bromine, which enhances the absorption rate by its increased lipid solubility and improves the pharmacological activity. It is also evident from the results obtained from structure-activity relationship (SAR) studies. Further, the photophysical properties of synthesized compounds were theoretical estimated using *ab-intio* technique. The ground state optimization and HOMO-LUMO energy levels are calculated using DFT-B3LYP-6-31G(d) basis set. Using theoretical estimated HOMO-LUMO value global chemical reactivity descriptors parameters are estimated and result shows synthesised molecule has highly electronegative and electrophilicity index. Overall results suggest that, fluorine substituted pyrazolones derivatives show good photophysical, SAR Studies and biological applications.

Keywords: Pyrazolones, *in-vitro and in-silico* biological activity, HOMO-LUMO, MESP

1. Introduction

Heterocyclic compounds are a highly valuable and unique class of compounds, exhibiting a broad spectrum of physical, chemical, and biological characteristics [1-2]. They are widely distributed in nature and play a significant role in metabolism, forming the structural nucleus of various natural products such as hormones, antibiotics, alkaloids, vitamins, and more [3-5]. Among heterocyclic compounds, nitrogen-containing heterocycles are prevalent and serve as a core framework in a diverse library of heterocycles, finding applications in natural and other scientific disciplines [6]. These nitrogen-containing heterocycles possess distinctive structural features and are commonly found in natural products, including vitamins, hormones, and alkaloids [7-8].

One notable family of nitrogen-containing compounds is pyrazole. Pyrazole derivatives display a wide range of biological activities, such as anti-tubercular, anti-AIDS, anti-malarial, anti-microbial, antitumor, anticancer, anti-fungal etc., [8-14]. Another compound, bipyrazole, has garnered significant attention due to its diuretic, cytotoxic, and cardiovascular efficacy. It is a privileged framework and serves as a bioactive component in commercially available medicines such as Floxan, pyrazomycin, difenamizole, and deramaxx. Additionally, bipyrazole finds applications in the paint and photographic industries and in the development of heat-resistant resins [15-20]. The corresponding 3-oxygenated derivative, pyrazolone 6, featuring an additional keto group, is a fundamental component in drugs like metamizole sodium and phenylbutazone. These drugs are non-steroidal anti-inflammatory medicines known for their potent painkilling and fever-reducing properties [15].

Furthermore, the benzo-fused derivative of pyrazole, known as tetrahydroindazole, is well-recognized for its biological activity and is utilized against cancer and inflammation [20-21]. Another important heterocyclic system in nature is indole, an isostere of indazole. Indole derivatives, such as serotonin and tryptophan, are essential neurotransmitters in the central nervous system [22]. Chemically, the basic structure of pyrazole consists of a five-membered ring with two nitrogen atoms at adjacent positions. Pyrazole has the molecular formula $C_3H_4N_2$, with six π electrons delocalized over the ring, forming an aromatic system. It is closely related to its reduced or oxidized forms, including pyrazoline, pyrazolidine, and pyrazolone. Unlike pyrazole, pyrazoline, and pyrazolidine are not considered aromatic compounds due to the absence of conjugation and delocalization of π electrons [23].

The goal of the present work is to synthesis of aryl substituted pyrazole molecule and estimate there biological and photophysical properties using experimental and theoretical technique.

2. **Materials and methods**

The reagents employed were of high purity commercial samples which were used as received (Fischer, Merck, and Sigma Aldrich). Reactions were carried out in an oven-dried RB flask. TLC was performed on alumina silica gel 60F254 (Fischer) detected by UV light (254 nm) and iodine vapors. The melting points were determined by open capillaries on a Buchi apparatus and are uncorrected. The IR spectra were recorded on a Nicolet-Impact-410 FT-IR spectrometer, using KBr pellets. ^{1}H-NMR and ^{13}C-NMR spectra were recorded on a Bruker AC-400F, 400MHz, spectrometer in DMSO-d_6 and $CDCl_3$ using TMS as an internal standard with the resonance frequency of 400 MHz and 100 MHz respectively. LCMS analyses were performed by using the Agilent 1200 series instrument. Elemental analysis was carried out by using Heraus CHN rapid analyzer. All the compounds gave C, H, and N analysis within ± 0.4% of the theoretical values.

2.1. **Synthesis of N/O-substituted pyrazalone derivatives**

The aryl substituted pyrazolone derivative ETH is synthesized as shown in Scheme 1. A highly functionalized adduct (3) was obtained by mixing 4-(trifluoromethyl)benzaldehyde (1) and activated propyl propionate (2) in the presence of a tertiary base. These adducts were converted to acetates ethyl 2-(hydroxy(4-(trifluoromethyl)phenyl)methyl)acrylate (3) in the presence a catalytic amount of pyridine and dichloromethane as the solvent. Further, ethyl 2-(acetoxy(4-(trifluoromethyl)phenyl)methyl)acrylate was treated with 3-methyl-1-phenyl-1H-pyrazol-5-ol to produce the desired target molecules (6). ^{1}H-NMR, LC-MS, and IR spectroscopy were used to confirm the synthesized compounds.

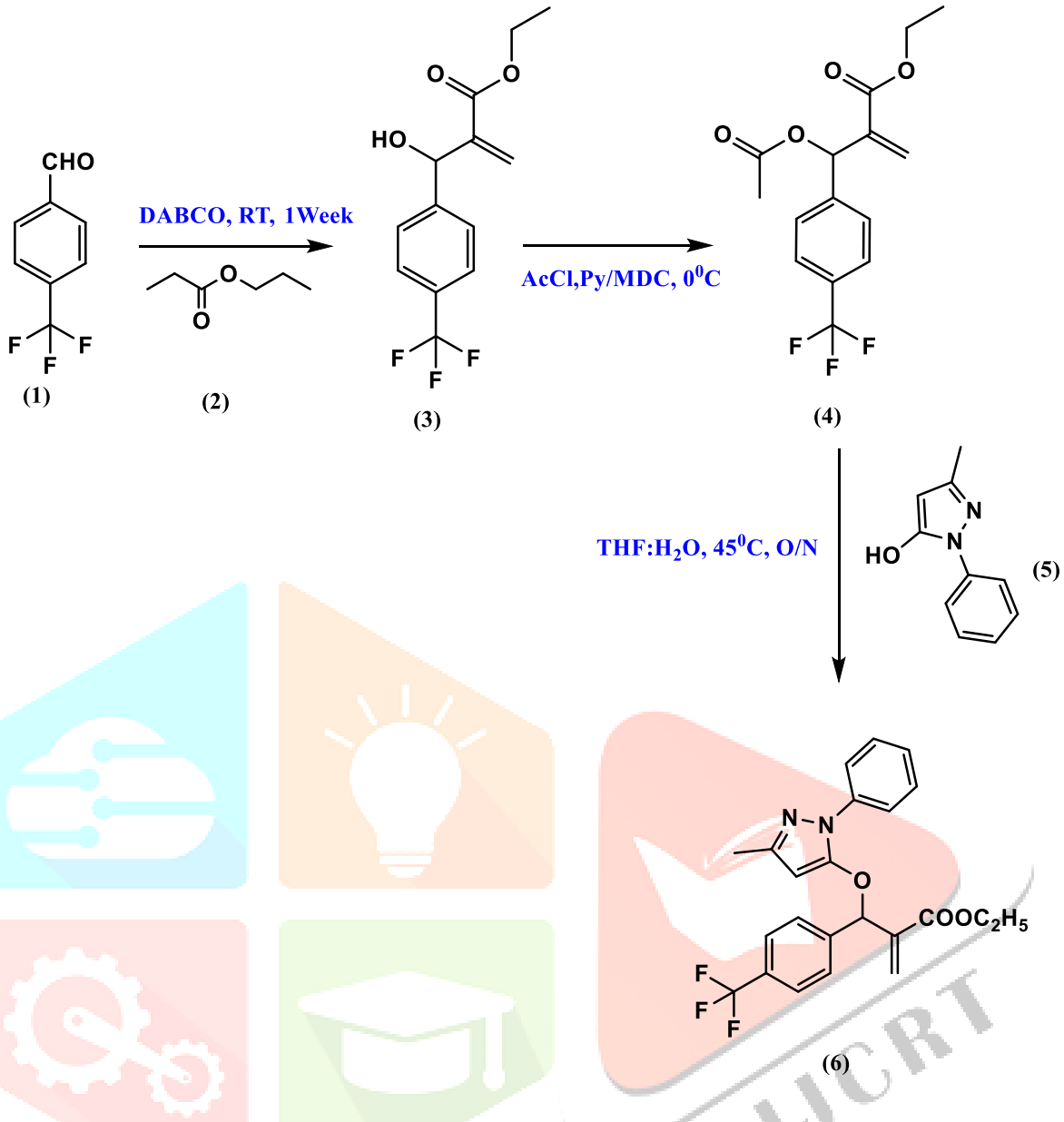

Scheme-1 synthesis of **ETH** molecule from Baylis-Hillman acetate.

2.2. **Structural characterization of the aryl-substituted pyrazolone (ETH)**

Colourless liquid, % yield: 45; ^{1}H NMR (300MHz, $CDCl_3$): δ= 7.47(m, 3H, Triazole, ArH), 7.45(m, 3H), 7.40(m, 4H), 7.26(m, 2H), 7.23(s, 1H, pyrazole), 4.01(m, 2H, CH_2), 1.9(s, 3H, CH_3), 1.22(t, 3H, CH_3); MS cald. for $C_{23}H_{21}F_3N_2O_3$: 430.15. Found: 431.2; IR (ν cm^{-1}): 2984(C-H), 1730(C=O); Elem. Anal. cald (found): C: 64.33(64.32), H: 4.69(4.65), N: 6.52(6.50).

3. Results and discussion

3.1. Computational photophysical studies

Molecular orbitals and their properties, including energy levels, serve as valuable tools for physicists and chemists. These orbitals, especially the frontier electron density, are instrumental in predicting the most reactive positions within π-electron systems and elucidating various reactions in conjugated systems [24-26]. Additionally, the eigenvalues of the highest occupied molecular orbital (HOMO) and the lowest unoccupied molecular orbital (LUMO), along with the energy gap between them, provide insights into the chemical reactivity of a molecule. Notably, the energy gap between the HOMO and LUMO has recently been employed to demonstrate the bioactivity resulting from intramolecular charge transfer (ICT) [27-28].

The ground state optimization of the newly synthesized aryl-substituted pyrazolone (ETH) was carried out using DFT-B3LYP/6-31G (d) basis set in Gaussian -09W software. The optimized molecular geometry and HOMO-LUMO energy plot of ETH were shown in Fig.1-2**.** From the HOMO-LUMO plot it is observed that, π–orbital of the HOMO electron cloud mainly distributes on 3-methyl-1-phenyl-1H-pyrazole and unfilled π^*–orbital LUMO is on ethyl 2-(4-(trifluoromethyl)benzyl)acrylate.

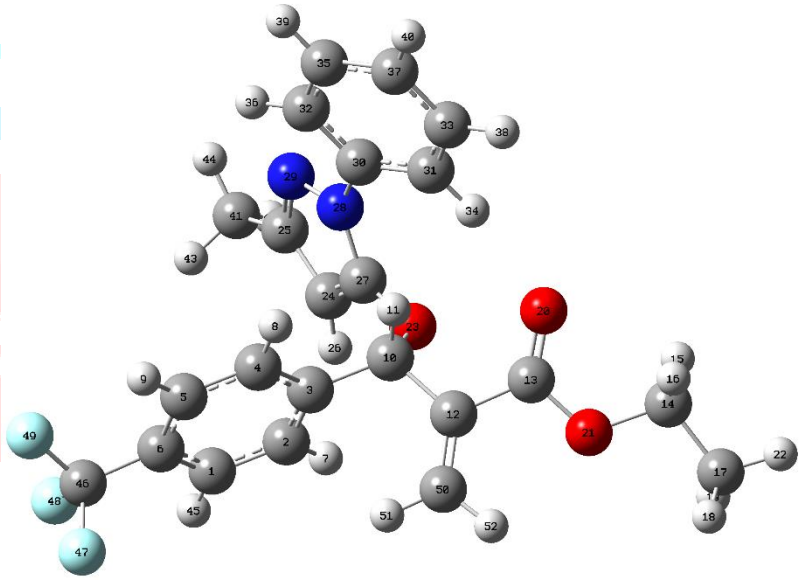

Fig.1. Optimised molecular geometry with atomic labels of the ETH molecule

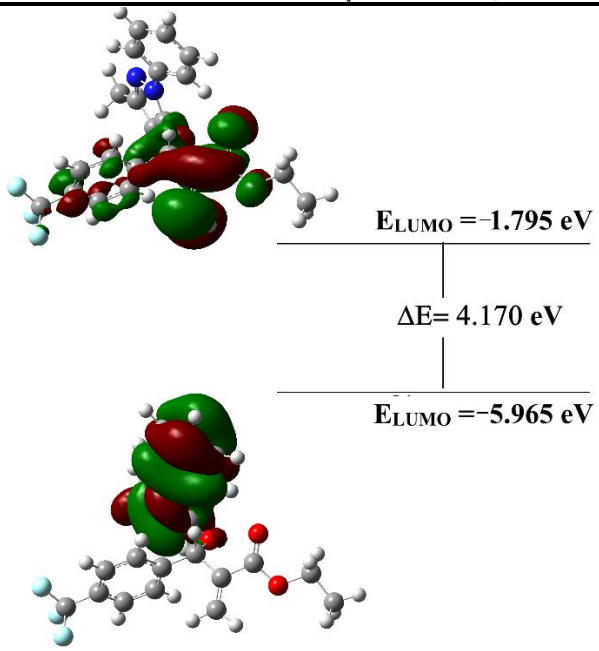

Fig.2. 3D plots of HOMO-LUMO with energy levels for ETH molecule

To gain insight on the chemical reactivity and stability of ETH molecules, global reactivity parameters [29], chemical hardness ($\eta = (IP - EA)/2$) =2.085 eV, electronegativity ($\chi = (IP + EA)/2$)= 3.880 eV, chemical potential ($\mu = -\chi$)= –3.880 eV, chemical softness ($S = 1/2\eta$)= 0.240 eV and electrophilicity index ($\omega = \mu^2/2\eta$) = 3.610 eV were calculated from E_{HOMO} and E_{LUMO} values [30], where, ionization potential, $IP = -E_{HOMO}$ = 5.965 eV and electron affinity, $EA = -E_{LUMO}$ = 1.795 eV. While a wider HOMO–LUMO gap is connected with stability and hardness, a lesser HOMO–LUMO gap signifies a more reactive soft molecule which is highly polarizable.

During molecular interactions, the lowest unoccupied molecular orbit (LUMO) accepts electrons and its energy corresponds to the electron affinity (EA = $-E_{LUMO}$), while the highest occupied molecular orbit (HOMO) represents electron donors, and its energy is associated with the ionization potential (IP = $-E_{HOMO}$). A molecule with a high frontier orbital gap (HOMO-LUMO energy gap) has a low chemical reactivity and high kinetic stability, because it is energetically unfavorable to add an electron to the high-lying LUMO in order to remove electrons from the low-lying HOMO. For instance, compounds that have a high HOMO-LUMO energy gap are stable, and hence are chemically harder than compounds having a small HOMO-LUMO energy gap. Thus, from GCRD parameter, that compound ETH is hard and more stable (less reactive) and it may be due to substitution of ethyl 2-(3-bromobenzyl) acrylate linked in non-planar to pyrozole and produce the highest energy gap. Thus, these substituents increase the reactivity of the five-membered ring.

The deformation of the molecular electron cloud is visible under mild perturbation due to the resistance that offers hardness throughout the chemical process. Hard molecules are comparatively small and significantly less polarizable than soft molecules, which are big and highly polarizable. The molecules stability and intermolecular reactivity are shown by the hardness. While softness exhibited an inverse effect with respect to hardness. The ability of additional electrical charge acquired by the electrophile is related to electrophilicity

phenomena. The information regarding chemical potential (electron transfer) and hardness of molecule (stability) were provided by the opposition to the exchange charge of an electron with nature. One of the most crucial quantum chemical descriptors for determining the toxicity of compounds in terms of their reactivity and site selectivity is the electrophilicity index [29]. According to HOMO-LUMO energy values, the electrophilicity index measures the reduction in energy brought on by the maximum amount of electron flow between the donor and acceptor. The lower value of ω indicated a good nucleophile, one with a higher ω value is considered a good electrophile. If any organic molecule is considered to be a strong electrophile the electrophilicity ω scale value should be $\omega > 1.5$ eV. If the scale varies between $0.8 < \omega < 1.5$ eV then those are considered as moderate electrophile and electrophile with electrophilicity value $\omega < 0.8$ eV are the weaker ones [30-31]. Our findings suggest that the ETH described here are better electrophiles because they have a higher value of ω. The propensity of electrons to leave a stable system is described as the chemical potential (μ). A complex has a negative chemical potential value if it is stable and does not spontaneously break into its constituent components. The ETH molecule does not break down into elements, as evidenced by their negative chemical potentials. The HOMO-LUMO gap support for chemical hardness at energy of 4.055 eV shows that this energy is less polarizable and resist the deformation of the chemical systems electron cloud under moderate disturbances.

3.2. Molecular electrostatic potential map (MESP)

The Molecular Electrostatic Potential (MESP) is a valuable parameter linked to electron density, offering insights into sites conducive to electrophilic and nucleophilic reactions, as well as hydrogen bonding interactions. Moreover, MESP is highly relevant for studying processes where one molecule interacts with another, such as in drug-receptor and enzyme-substrate interactions. This interaction begins with the recognition of the two species through their electrostatic potentials. To pinpoint the reactive sites for electrophilic and nucleophilic attacks in the molecule under investigation, we calculated the MESP at the optimized geometry using DFT-B3LYP/6-31G(d). Different colors on the MESP surface correspond to distinct electrostatic potential values: red indicates regions with the most negative potential, blue represents the most positive regions, and green signifies areas with zero electrostatic potential. Negative electrostatic potential, characterized by shades of red, indicates regions where protons are attracted to the electron density within the molecule. In contrast, positive electrostatic potential, seen in shades of blue, indicates regions where protons are repelled by atomic nuclei. Specifically, the negative (red and yellow) regions of the MEP denote electrophilic reactivity, while the positive (blue) regions signify nucleophilic reactivity (see Fig. 3). Upon examining the MEP, it becomes evident that the negative charge predominantly covers the ethyl methacrylate, while the positive region is concentrated over the hydroxyl group and the N-H section. The higher electronegativity of the nitro group renders it the most reactive part of the molecule [32].

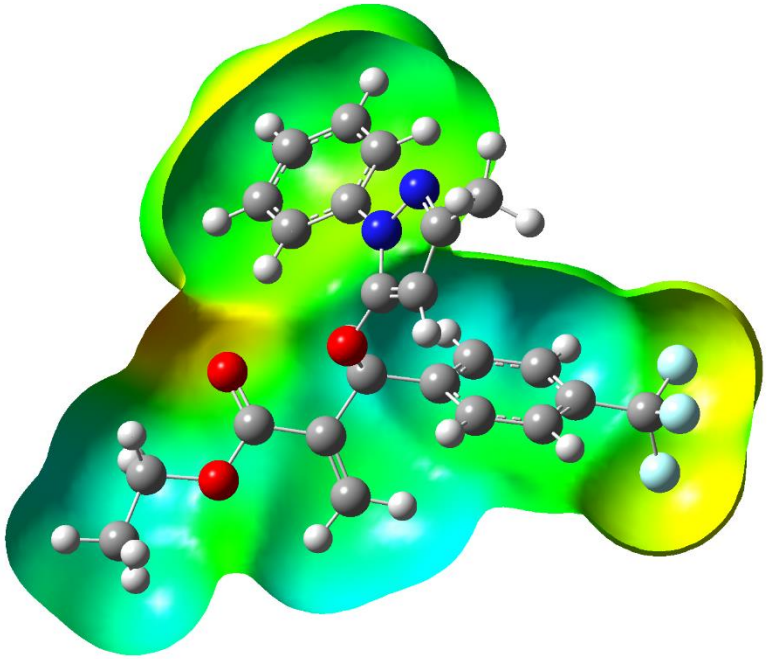

Fig.3. Molecular electrostatic potential map of ETH molecule

3.3. **In vitro antimicrobial, antifungal, and antioxidant activity**

The newly synthesized molecule ETH were subjected to antimicrobial studies and interestingly, the compound exhibited perfect antibacterial activity against *S.aureus, B.subtillis, S.typhi,* and *E.coli* and details are given in Table-1. In addition, ETH molecule also exhibited very good antifungal activity against *A. niger* and *C. Albicans and* details are given Table 1. The better activity of the products could be due to the presence of biologically active pyrazole and bromo benzene ring. Bromobenzene is the second smallest substituent, which resembles hydrogen with respect to steric requirements at enzyme receptor sites. The presence of bromine enhances the absorption rate by its increased lipid solubility [33]. The high lipophilic character of the bromobenzene group is significant in improving pharmacological activity. Further, antioxidant activity of the ETH molecules was screened and showed excellent radical scavenging capacity at the tested concentration of 15 μg/mL in comparison with the standard edaravone as shown in Table 2. The variation exhibited in DPPH scavenging capacity could be attributed to the effect of different substitutions at 1, 2, 3 and 5 of the synthesized compounds. The antioxidant activity results are in the range as observed in the previous results [34].

Table -1 Antimicrobial and antifungal activity of the newly synthesized pyrazolones derivatives

Compound	*S. aureus*	*B. subtilis*	*S. typhi*	*E. coli*	*A. niger*	*C. albicans*
ETH	26(20)	27(30)	26(40)	30(20)	24(30)	20(40)
Standard[a]	24	23	23	25	25	24
Control[b] DMSO	0	0	0	0	0	0

Note: [a]Standard drug used: Bacteria (Ciprofloxacin), Fungal (Fluconazole) were in 40 µg in 100µL, and R: Resistance
[b]Control: DMSO (Dimethyl sulphoxide)

Table-2 DPPH scavenging assay of aryl substituted pyrazolones derivatives.

Compounds Concentration (15µg/mL)	ETH	Standard (edaravone)
% DPPH scavenging	47.11	73.16

4. **Conclusions**

In the present work, we synthesised highly functionalized aryl-substituted pyrazolone derivatives (ETH). The physicochemical properties of the ETH are confirmed by ^{1}H-NMR, FT-IR and LC-MS data. The photophysical properties of the compounds were comprehensively estimated using computational technique. The optimised molecular geometry, HOMO-LUMO and MESP plot of the ETH molecule are estimated using DFT-B3LYP-6-31G(d) basis set. Using theoretical estimated HOMO-LUMO values global chemical reactive descriptor parameters is estimated and results shows that ETH molecule has a good electrophile, highlighting its reactivity and relatively lower stability. Electron-deficient sites in ETH were identified through DFT computational studies, which can be utilized in the design of drugs for biological applications. Furthermore, the *in-vitro* antimicrobial, antifungal and antioxidant activities of the ETH molecule was examined and results shows that molecule has high biological application. Additionally, *in-silico* molecular docking studies showed the synthesised molecule has better interactions with the target receptors like ciprofloxacin, fluconazole and edaravone in the range of -10.0 to -8.5 (kcal/mol) than the medicinal standard drug *Rifampicin* (-8.6kcal/mol). The synthesised molecule will be able to exhibit our initiative by serving as effective molecules in drug design. These could be helpful in regulating pathogen-abnormal behavior. Overall, the results indicate that the ETH could be used as biological applications.

Acknowledgments.

The authors express their gratitude for the encouragement and support received from M.G.V.C. Arts Commerce and Science College in Muddebihal, Vijayapur , Karnataka, India.

Reference

1. Breijyeh, Z., Jubeh, B., & Karaman, R. Resistance of gram-negative bacteria to current antibacterial agents and approaches to resolve it. *Molecules*, *25*(6), (2020) 1340.
2. Balasubramaniam, B., Prateek, Ranjan, S., Saraf, M., Kar, P., Singh, S. P., & Gupta, R. K. Antibacterial and antiviral functional materials: chemistry and biological activity toward tackling COVID-19-like pandemics. *ACS Pharmacology & Translational Science*, *4*(1), (2020) 8.
3. Nasir, N., Rehman, F., & Omair, S. F. Risk factors for bacterial infections in patients with moderate to severe COVID-19: A case-control study. *Journal of medical virology*, *93*(7), (2021) 4564.
4. Becerra, D., Abonia, R., & Castillo, J. C. Recent applications of the multicomponent synthesis for bioactive pyrazole derivatives. Molecules, 27(15), (2022) 4723
5. Özlem, U. Ğ. U. Z., Gümüş, M., Yusuf, S. E. R. T., İrfan, K. O. C. A., & Atıf, K. O. C. A. Utilization of pyrazole-perimidine hybrids bearing different substituents as corrosion inhibitors for 304 stainless steel in acidic media. Journal of Molecular Structure, 1262, (2022) 133025.
6. Özkınalı, S., Gür, M., Şener, N., Alkın, S., & Çavuş, M. S. Synthesis of new azo schiff bases of pyrazole derivatives and their spectroscopic and theoretical investigations. Journal of Molecular Structure, 1174, (2018). 74-83.
7. Khoram, M. M., Nematollahi, D., Momeni, S., Zarei, M., & Zolfigol, M. A. Electrochemical study of dibenzo-xanthene and dihydrobenzochromono pyrazole derivatives. Electrochimica Acta, 326, (2019) 134990.
8. Gao, M., Qu, K., Zhang, W., & Wang, X. Pharmacological activity of pyrazole derivatives as an anticonvulsant for benefit against epilepsy. *Neuroimmunomodulation*, *28*(2), (2021) 90.
9. Santos, N. E., Carreira, A. R., Silva, V. L., & Braga, S. S. Natural and biomimetic antitumor pyrazoles, a perspective. *Molecules*, *25*(6), (2020) 1364.
10. Datar, P. A., & Jadhav, S. R. Design and synthesis of pyrazole-3-one derivatives as hypoglycaemic agents. *International Journal of Medicinal Chemistry*, *2015* (2015).
11. Cetin, A., & Bildirici, I. A study on synthesis and antimicrobial activity of 4-acyl-pyrazoles. *Journal of Saudi Chemical Society*, *22*(3), (2018) 279.
12. Uramaru, N., Shigematsu, H., Toda, A., Eyanagi, R., Kitamura, S., & Ohta, S. Design, synthesis, and pharmacological activity of nonallergenic pyrazolone-type antipyretic analgesics. *Journal of medicinal chemistry*, *53*(24), (2010) 8727.
13. Desideri, N., Fioravanti, R., Proietti Monaco, L., Atzori, E. M., Carta, A., Delogu, I., & Loddo, R. Design, Synthesis, Antiviral evaluation, and SAR studies of new 1-(phenylsulfonyl)-1 H-pyrazol− 4-yl-methylaniline derivatives. *Frontiers in chemistry*, *7*, (2019) 214.
14. Pandya, K. M., Patel, A. H., & Desai, P. S. Development of Antimicrobial, Antimalarial and Antitubercular Compounds Based on a quinoline-pyrazole clubbed scaffold derived via Doebner reaction. *Chemistry Africa*, *3*, (2020) 89.

15. Zalaru, C., Dumitrascu, F., Draghici, C., Iovu, M., Marinescu, M., Tarcomnicu, I., Nitulescu, G.M. Synthesis and biological screening of some novel 2-(1H-pyrazol-1-yl)-acetamides as lidocaine analogue. *Indian J. Chem. B* 53, (2014) 733
16. Refat, M. S., Hamza, R. Z., Adam, A. M. A., Saad, H. A., Gobouri, A. A., Al-Salmi, F. A., & El-Megharbel, S. M. Synthesis of N, N′-bis (1, 5-dimethyl-2-phenyl-1, 2-dihydro-3-oxopyrazol-4-yl) sebacamide that ameliorate osteoarthritis symptoms and improve bone marrow matrix structure and cartilage alterations induced by monoiodoacetate in the rat model:"Suggested potent anti-inflammatory agent against COVID-19". *Human & Experimental Toxicology*, *40*(2), (2021) 325.
17. Flamholc, R., Zakrzewski, J., Makal, A., Brosseau, A., & Métivier, R. Synthesis, regioselective aerobic Pd (II)-catalyzed C–H bond alkenylation and the photophysical properties of pyrenylphenylpyrazoles. *Photochemical & Photobiological Sciences*, *15*(4), (2016) 580.
18. Castillo, J. C., & Portilla, J. Recent advances in the synthesis of new pyrazole derivatives. *Targets Heterocycl. Syst*, *22*, (2018) 194.
19. Beillard, A., Bantreil, X., Métro, T. X., Martinez, J., & Lamaty, F. Alternative technologies that facilitate access to discrete metal complexes. *Chemical reviews*, *119*(12), (2019) 7529.
20. Beneto, A. J., & Siva, A. Highly selective colorimetric detection of cyanide anions in aqueous media by triphenylamine and phenanthro (9, 10-d) imidazole based probes. *Photochemical & Photobiological Sciences*, *16*, (2017) 255.
21. Naskar, B., Das, K., Mondal, R. R., Maiti, D. K., Requena, A., Cerón-Carrasco, J. P., & Goswami, S. A new fluorescence turn-on chemosensor for nanomolar detection of Al^{3+} constructed from a pyridine–pyrazole system. *New Journal of Chemistry*, *42*(4), (2018) 2933.
22. A.H. Collins, Microbiological Methods, 2nd Edition, Butterworth, London, 1976.
23. Arthington-Skaggs, B. A., Motley, M., Warnock, D. W., & Morrison, C. J. Comparative evaluation of PASCO and national committee for clinical laboratory standards M27-A broth microdilution methods for antifungal drug susceptibility testing of yeasts. *Journal of Clinical Microbiology*, *38*(6), (2000) 2254.
24. Naik, L., Maridevarmath, C. V., Khazi, I. A. M., & Malimath, G. H. Photophysical and computational studies on optoelectronically active thiophene substituted 1, 3, 4-oxadiazole derivatives. *Journal of Photochemistry and Photobiology A: Chemistry*, *368*, (2019) 200
25. Walki, S., Malimath, G. H., Mahadevan, K. M., Naik, S., Sutar, S. M., Savanur, H., & Naik, L. Synthesis, spectroscopic properties, and DFT correlative studies of 3, 3′-carbonyl biscoumarin derivatives. *Journal of Molecular Structure*, *1243*, (2021). 130781.
26. Prabhala, P., Sutar, S. M., Manjunatha, M. R., Pawashe, G. M., Gupta, V. K., Naik, L., & Kalkhambkar, R. G. Synthesis, in vitro and theoretical studies on newly synthesized deep blue emitting 4-(p-methylphenylsulfonyl-5-aryl/alkyl) oxazole analogues for biological and optoelectronic applications. *Journal of Molecular Liquids*, *360*, (2022) 119520.

27. Naik, L., Thippeswamy, M. S., Praveenkumar, V., Malimath, G. H., Ramesh, D., Sutar, S., & Bubbly, S. G. Solute-solvent interaction and DFT studies on bromonaphthofuran 1, 3, 4-oxadiazole fluorophores for optoelectronic applications. *Journal of Molecular Graphics and Modelling*, *118*, (2023) 108367.

28. Calais, J. L. (1993). Density-functional theory of atoms and molecules. RG Parr and W. Yang, Oxford University press, New York, Oxford, *International Journal of Quantum Chemistry*, *47*(1), (1989) 101.

29. Choudhary, V., Bhatt, A., Dash, D., & Sharma, N. DFT calculations on molecular structures, HOMO–LUMO study, reactivity descriptors and spectral analyses of newly synthesized diorganotin (IV) 2-chloridophenylacetohydroxamate complexes. *Journal of computational chemistry*, *40*(27), (2019) 2354.

30. Yankova, R., & Tankov, I. NLO response as a function of structural water presence: A comparative experimental (UV-vis) and DFT (structural, NPA, MEP) study on Cs_2Ni (SeO_4) 2• $4H_2O$ and Cs_2Ni (SeO_4) 2. *Journal of Molecular Structure*, *1224*, (2021) 129047.

31. Glendening, E. D., Reed, A. E., Carpenter, J. E., & Weinhold, F. NBO, version 3.1, Gaussian. *Inc.: Pittsburgh, PA* (2003).

32. Foster, A. J., & Weinhold, F. Natural hybrid orbitals. *Journal of the American Chemical Society*, *102*(24), (1980) 7211.

33. Domingo, L. R., Ríos-Gutiérrez, M., & Pérez, P. Applications of the conceptual density functional theory indices to organic chemistry reactivity. *Molecules*, *21*(6), (2016) 748.

Supplementary files

Compounds	Pyrazolone	Baylis-Hillman acetate	Product
ETH	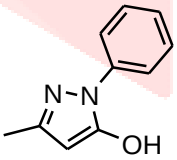	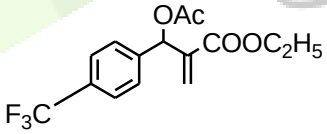	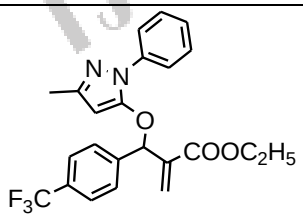

In vitro antifungal studies

Newly synthesized pyrazolones were screened for their antifungal activity against A. niger and C. Albicans in DMSO by the serial plate dilution method. Sabourand agar media was prepared by dissolving peptone (1g), D-glucose (4g), and agar (2g) in distilled water (100 ml), and the pH was adjusted to 5.7. Normal saline was used to make a suspension of spores of fungal strain for lawning. A loopful of a particular fungal strain was transferred to 3 mL of saline to get a suspension of the corresponding species. Agar media of 20 mL was poured into each Petri dish. An excess of suspension was decanted, and the plates were dried by placing them in an incubator at 37 °C for 1h. Using an agar, punch wells were made on these seeded agar plates, and 10 µg/mL-50 µg/mL of the test compounds in DMSO were added to each well labeled. A control was also prepared for plates, in the same way, using the solvent DMSO. The Petri dishes were prepared in triplicate and maintained at 37°C for 3-4 days. Antifungal activity was determined by measuring the inhibition zone. The results were compared with those of the standard Fluconazole.

In vitro antibacterial studies

The newly synthesized pyrazolones were also screened for their antibacterial activity against S. aureus, B. subtilis, E. coli, and S. typhi bacterial strains by the disc diffusion method. The discs measuring 6.25 mm in diameter were punched from the Whatman No.1 filter paper. Batches of 100 discs were dispensed into each screw-capped bottle and sterilized by dry heat at 140 °C for an hour. The test compounds were prepared at different concentrations using dimethyl sulfoxide (DMSO). A 1mL container containing 100 times the amount of chemical in each disc was added to each bottle, which contained 100 discs. The discs of each concentration were placed in triplicate in a nutrient agar medium separately seeded with fresh bacteria. The incubation was carried out at 37°C for 24 h. Solvent and growth controls were kept, and the zones of inhibition and minimum inhibitory concentrations were noted. The results were compared with those of the standard Ciprofloxacin.

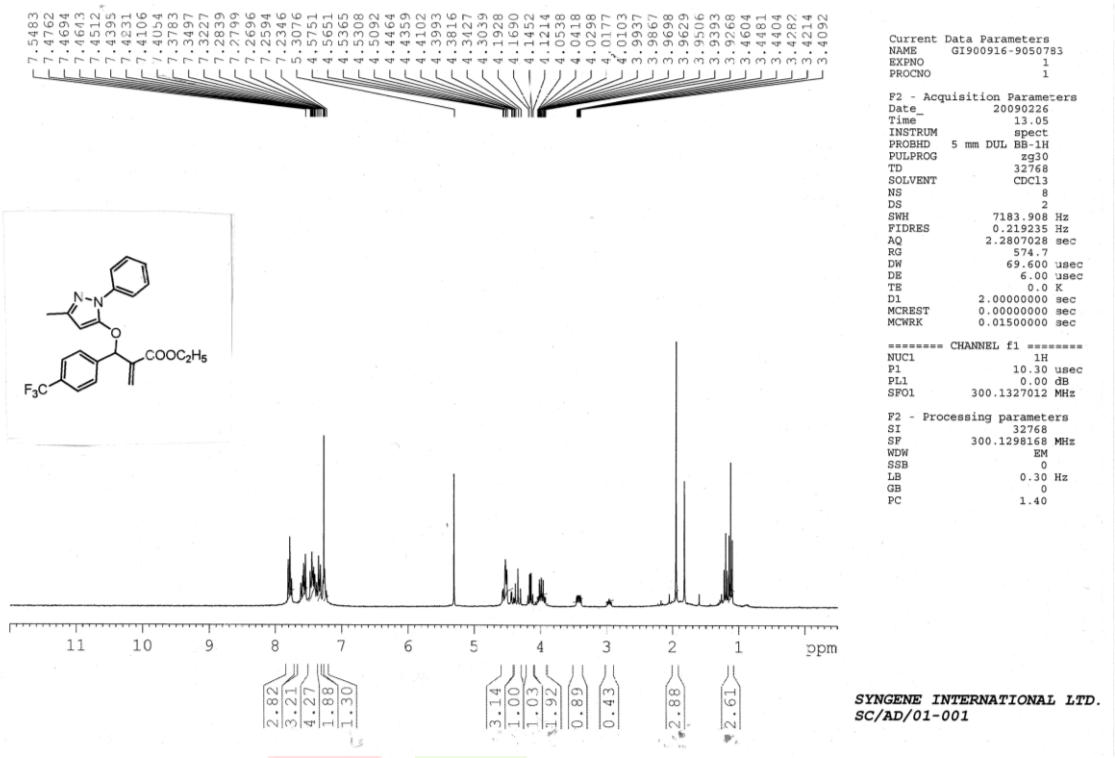

Fig.s1 ^{1}H-NMR spectra of ETH

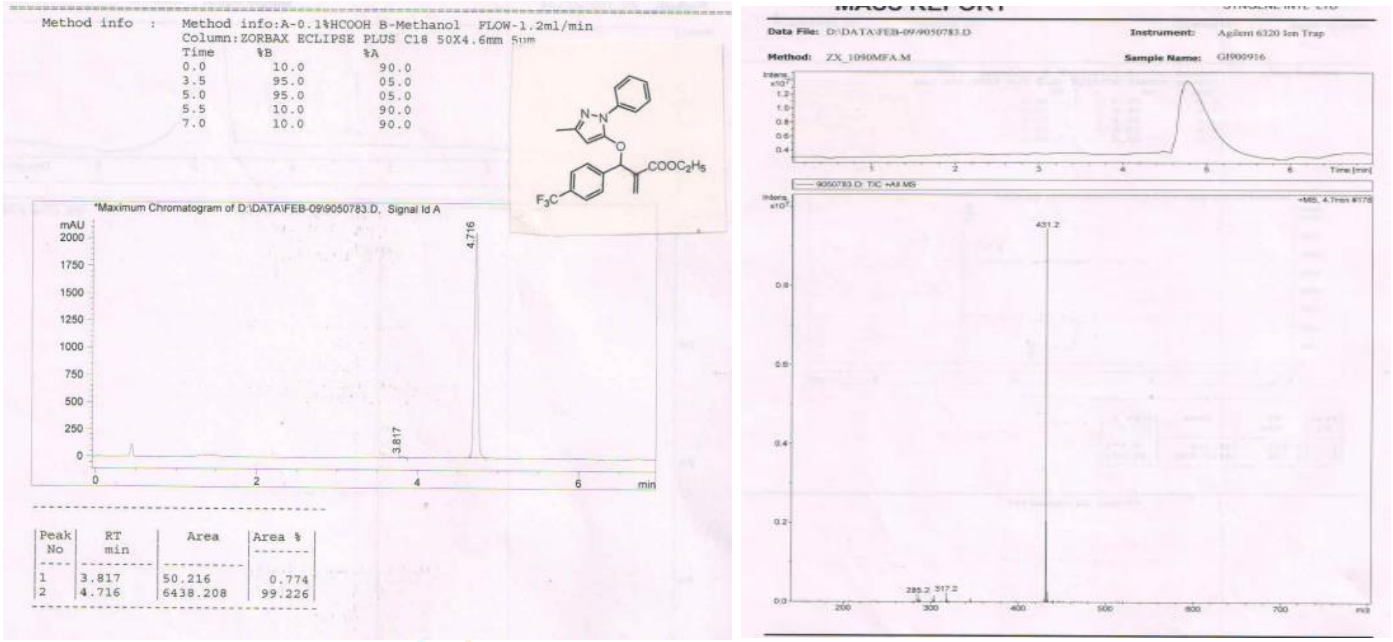

Fig.s2 LC-MS spectra of ETH

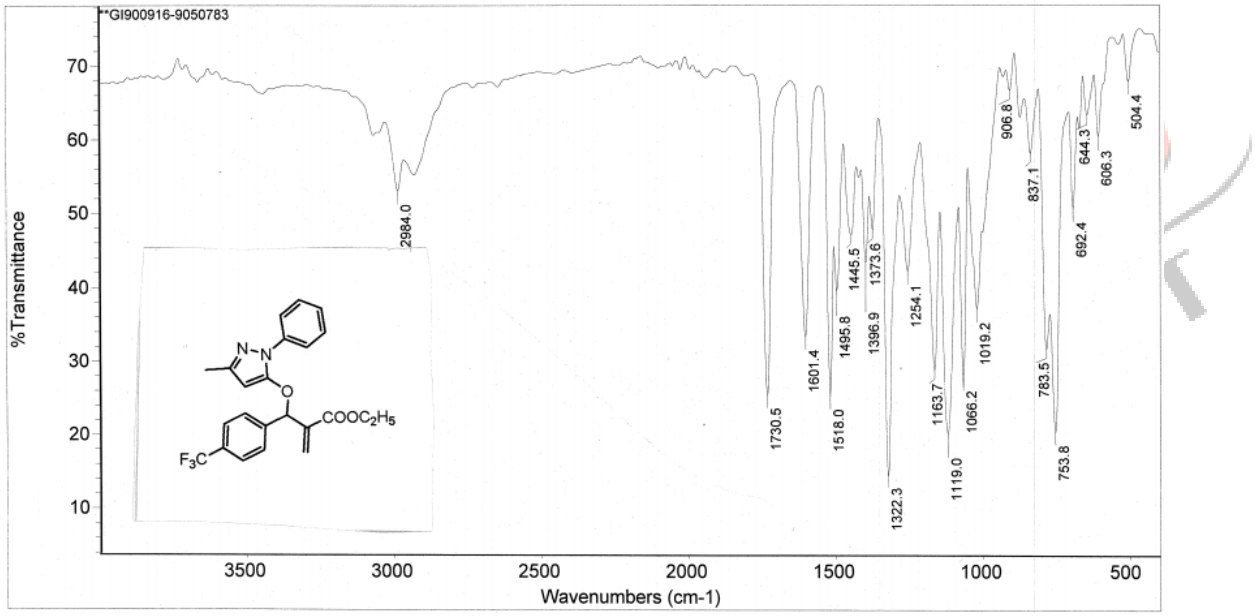

Fig.s3 FT-IR spectra of ETH